Journal of Natural Fibers

ISSN: (Print) (Online) Journal homepage: https://www.tandfonline.com/loi/wjnf20

Reactive Blue 21 Exhaustion Degree Investigated Using the Surface Response Methodology as an Auxiliary Tool in Cotton Dyeing

Jorge Marcos Rosa, Camila Gomes Melo, Maria Da Conceição Costa Pereira & Sueli Ivone Borrely

To cite this article: Jorge Marcos Rosa, Camila Gomes Melo, Maria Da Conceição Costa Pereira & Sueli Ivone Borrely (2021) Reactive Blue 21 Exhaustion Degree Investigated Using the Surface Response Methodology as an Auxiliary Tool in Cotton Dyeing, Journal of Natural Fibers, 18:4, 520-530, DOI: 10.1080/15440478.2019.1636739

To link to this article: https://doi.org/10.1080/15440478.2019.1636739

JOURNAL OF NATURAL FIBERS
2021, VOL. 18, NO. 4, 520–530
https://doi.org/10.1080/15440478.2019.1636739

Taylor & Francis
Taylor & Francis Group

REVIEW

Reactive Blue 21 Exhaustion Degree Investigated Using the Surface Response Methodology as an Auxiliary Tool in Cotton Dyeing

Jorge Marcos Rosa [a,b,c], Camila Gomes Melo[c], Maria Da Conceição Costa Pereira[c], and Sueli Ivone Borrely [c]

[a]Department of Textile Chemistry, College of Technology SENAI "Antoine Skaf", São Paulo, Brazil; [b]College of Chemical Engineering, State University of Campinas, Campinas, Brazil; [c]Radiation Technology Center, Nuclear and Energy Research Institute, IPEN-CNEN/SP, São Paulo, Brazil

ABSTRACT

Response surface methodology was used to investigate the influences of sodium chloride (NaCl), soda ash (Na_2CO_3), and sodium hydroxide (NaOH) concentrations on cotton and the degree of exhaustion (D_E) of Reactive Blue 21 dyestuff (RB21), as well as to optimize dyeing conditions. A 2^3 central composite and rotational design was used as a support to carry out 17 dyeings with RB21 on a 100% knitted cotton substrate. NaCl, Na_2CO_3, and NaOH concentrations were used as factors. Responses comprised color strength (K S ^{1}) and the D_E. The results indicate that a square model was the best fit. This model was able to increase both K S ^{1} and D_E values, with the color-fastness to water and rubbing carried out with supplier's formulation recipe. This study demonstrates that the use of the response surface methodology in color matching can contribute to the textile industry in the prediction or assessment of formulations for a specific color.

摘要

采用响应面法研究了氯化钠（NaCl）、纯碱（Na2CO3）、氢氧化钠（NaOH）浓度对棉纤维的影响，以及活性蓝21染料（RB21）的消耗程度（DE），并对染色条件进行了优化.以23中心复合旋转设计（CCRD）为载体，在100%针织棉基材上用RB21进行17次染色.以NaCl、Na2CO3和NaOH浓度作为影响因素.响应包括颜色强度（k s 1）和DE. 结果表明，方形模型最适合.该模型能够提高K S 1和De值，并根据供应商的配方进行耐水和摩擦色牢度试验.这项研究表明，在颜色匹配中使用响应面方法有助于纺织行业预测或评估特定颜色的配方.

KEYWORDS
Degree of exhaustion; response surface methodology; color strength; cotton dyeing; Reactive Blue 21; textile industry

关键词
疲劳程度; 响应面方法; 颜色强度; 棉花染色; 反应蓝21; 纺织工业

Introduction

The textile chain had comprised of approximately US$45 billion, the equivalent of 7% of the total production value of the manufacturing industry. Jobs generated by the Brazilian textile chain totaled 1.5 million in 2016, or 18.7% of the total industrial production workforce, almost a quarter of the workforce employed in the manufacturing industry, reinforcing the sector's importance for the economy in general. This sector is also responsible for a large part of the economy in many developed countries and is one of the main economic activities of some developing countries (Prado 2018; Rosa et al. 2014).

CONTACT Jorge Marcos Rosa jotarosa@hotmail.com Department of Textile Chemistry, College of Technology SENAI "Antoine Skaf", Correia de Andrade Street, 232, CEP, Sao Paulo 03008-020, Brazil

Color versions of one or more of the figures in the article can be found online at www.tandfonline.com/wjnf.

Among all dyed textile fibers, cotton is the most commonly used, and over 50% of the cotton produced worldwide is dyed with reactive dyestuff. Nitrogen fibers, such as wool and silk, are also dyed with reactive dyestuffs. It is estimated that approximately 10–60% of this kind of dyestuff are lost during textile dyeing, producing large amounts of colored effluents (Farzana et al. 2018; Hallas 2002; Shu et al. 2018; Siddiqua et al. 2017).

Dyestuff

The reactive dyestuff assessed in this study, Reactive Blue 21 (RB21 – CAS number 12236-86-1), has a molecular weight of 1079.53 g mol^{-1}, consisting of a homo-functional, vinylsulphone reactive group and with a phthalocyanine as chromophore group (Zollinger 2003). Various methods involving adsorption techniques have been developed for the treatment of effluents containing RB21 (Ma and Wang 2015; Vanaamudan, Chavada, and Padmaja 2016; Vanaamudan, Pathan, and Pamidimukkala 2014), mainly due to the complexity of its structure, which is demonstrated in Figure 1.

Response surface methodology

Among the various system optimization techniques available, response surface methodology (RSM) has been highlighted, due to its fast and easy manner of presenting the maximum (or minimum) conditions of an empirical model, as regions on a hypersurface (Bordin et al. 2018).

Many studies applying RSM and other mathematical tools have been carried out in the textile area. However, most of them involve effluent treatment in order to find an efficient approach to simulate different processes for the degradation of many types of dyestuffs or their effluents (Mokhtar et al. 2016; Ngwabebhoh, Gazi, and Oladipo 2016; Torbati, Khataee, and Movafeghi 2014).

In this context, the importance of optimizing dyeing processes with this class of dyestuff in order to obtain higher color strength levels becomes evident, minimizing salt and dyestuff discharges and promoting lower amounts of pollutants in the generated effluent (Rosa and Fileti 2016).

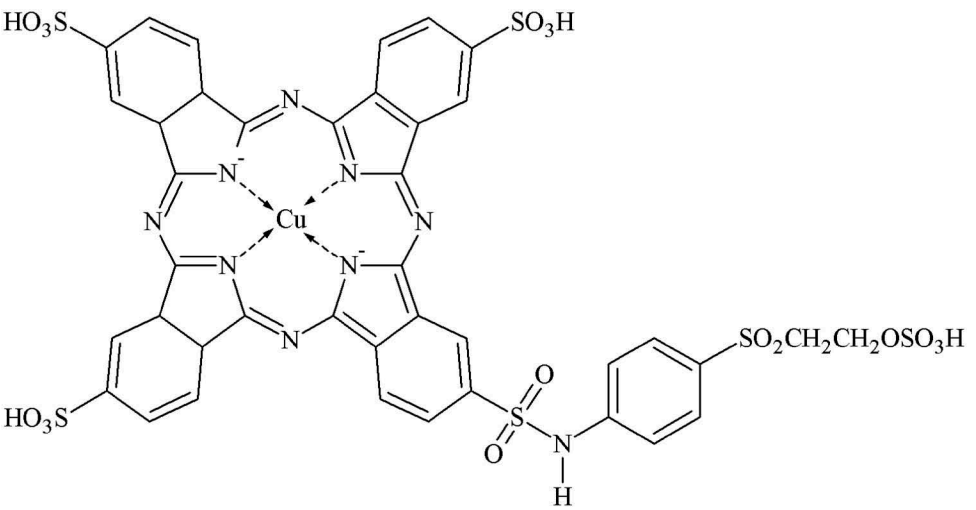

Figure 1. RB21 structure (Ma and Wang 2015; Zollinger 2003).

This study aimed to apply the RSM to analyze the influences of three independent variables used in the cotton reactive dyeing process and optimize its application. Thus, a 2^3 central composite and rotational design was used to verify the influences of the sodium chloride (NaCl), sodium carbonate (Na_2CO_3), and NaOH 50 °Bé concentrations on color strength ($K\ S^{-1}$). $K\ S^{-1}$ is calculated by the Kubelka–Munk equation (Equation 1) (Shen, Ya, and Ji-Huan 2016; Zurita Ares et al. 2016), as follows:

$$K\ S^{-1} = \frac{(1-R)^2}{2R} \tag{1}$$

Reflectation (R) values were determined by visible spectrophotometry, under a D_{65} illuminant, 10° (Konica-Minolta CM 3600d).

Methodology

Dyeing procedure

A total of 17 cotton samples at 5 g each (150 g m^{-2} poplin cotton supplied by SENAI-SP)were bleached according to the process described by Rosa et al. (2015) and dyed according to dyestuff supplier recommendations (Golden Technology). A Mathis Alt-1 equipment, at 10:1 of liquor ratio, was used. All steps of the dyeing process are displayed in Figure 2.

After the bleaching step, the total NaCl amount was added to the mixture (A, supplied by SENAI-SP). Subsequently, 1.5% of RB21 (B, supplied by Golden Technology), calculated using fiber weight (% owf), was added. After 10 min, the temperature was raised up to 60°C. The Na_2CO_3 and NaOH 50 °Bé mixture (C, both supplied by SENAI-SP) was introduced in the bath by linear dosing during 15 min. Then, the dyeing process was performed at 60°C for 60 min. Finally, the samples were washed off three times in water at 25°C, followed by a bath containing 1.0 g L^{-1} nonionic dispersant (D, supplied by Golden Technology) applied at 95°C during 10 min and washed off with water at 25°C. Deionized water was used in all steps, and all chemicals were used without previous purification.

RSM application

Table 1 displays the independent factors, their corresponding values, and the three factors that were varied at these five levels (−2, −1, 0, +1, and +2). The factor levels of the investigated variables were

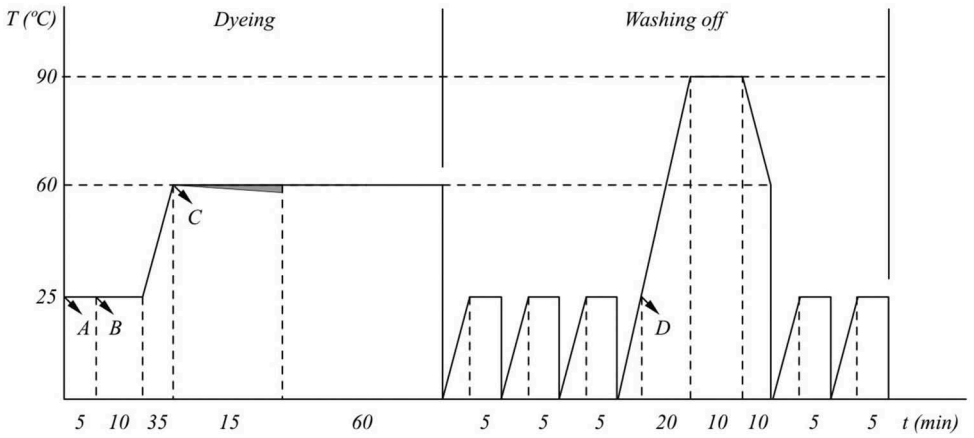

Figure 2. Process of dyeing.

Table 1. Independents variables.

N	X1	NaCl	X2	Na_2CO_3	X3	NaOH
1	−1	35	−1	7.5	−1	0.25
2	1	65	−1	7.5	−1	0.25
3	−1	35	1	12.5	−1	0.25
4	1	65	1	12.5	−1	0.25
5	−1	35	−1	7.5	1	0.75
6	1	65	−1	7.5	1	0.75
7	−1	35	1	12.5	1	0.75
8	1	65	1	12.5	1	0.75
9	−2	20	0	10	0	0.5
10	2	80	0	10	0	0.5
11	0	50	−2	5	0	0.5
12	0	50	2	15	0	0.5
13	0	50	0	10	−2	0
14	0	50	0	10	2	1
15	0	50	0	10	0	0.5
16	0	50	0	10	0	0.5
17	0	50	0	10	0	0.5

chosen by considering the preliminary tests on the effect of individual variables on dyeing and operating limits in order to obtain the best K S^{-1} conditions.

The square response surface model, which considered the linear, hyperbolic, and square interaction effects of the variables, was applied to preliminary regression fits, through Equation 2 (Ezekannagha, Ude, and Onukwuli 2017).

$$Y = \beta_0 + \sum_{i=1}^{n} \beta_i x_i + \sum_{i=1}^{n} \beta_{ii} x_i^2 + \sum_{i=1}^{n-1} \sum_{j=i+1}^{n} \beta_{ij} x_j x_j \quad (2)$$

where Y = response factor (K S^{-1}), x_i = independent factor term, β_0 = intercept, β_i = linear model coefficient, β_{ii} = quadratic coefficient for the factor i, and β_{ij} = linear model coefficient for the interaction between factors i and j.

Model fit was assessed by an analysis of variance (ANOVA) and optimization was assessed by RSM, both using the Statistica 13® software. The ANOVA test is employed for the determination of significant variables, consisting of classifying and cross-classifying statistical results and was tested by the means of a specified classification difference, carried out by Fisher's statistical test (F-test). The F-value is defined as the ratio of the mean square of regression (MRR) to the error (MRe) (F = MRR/MRe), representing the significance of each controlled variable on the tested model (Santana et al. 2018; Campos Benvenga et al. 2016; Sathish and Vivekanandan 2016). For a model to be considered fitted, the calculated $F1$ must be greater than or equal to the tabulated F1, while the R^2 value should be close to 1 (Das and Mishra 2017).

Degree of exhaustion

In order to calculate the degree of exhaustion (D_E) of the dyeings, a 1.5 g L^{-1} of RB21 solution ($[RB21_o]$) was prepared. This initial solution was diluted in 10 aliquots (100%, 90%, 80%, 70%, 60%, 50%, 40%, 30%, 20% and 10%) in order to determinate the final concentration of RB21 ($[RB21_f]$). Solution absorbances (Abs) were evaluated using acrylic 1.0-cm optical path cuvettes by visible spectrophotometry (Konica Minolta CM 3600d). The data are described in Table 2.

A theoretical calibration curve (Figure 3) was developed applying the absorbance values and solution concentrations, resulting in Equation 3.

$$[RB21]_n = \frac{Abs_n - 0.1094}{3.8813} \quad (3)$$

Table 2. Solutions and its absorbance values.

[RB21]	%	[RB21] (g L^{-1})	Abs (610 nm)
Initial	100	1.50	5.8958
-	90	1.35	5.3076
-	80	1.20	4.7193
-	70	1.05	4.0891
-	60	0.90	3.6880
-	50	0.75	3.1312
-	40	0.60	2.6086
-	30	0.45	1.8882
-	20	0.30	1.2781
-	10	0.15	0.6181
Final	0	0.00	0.0000

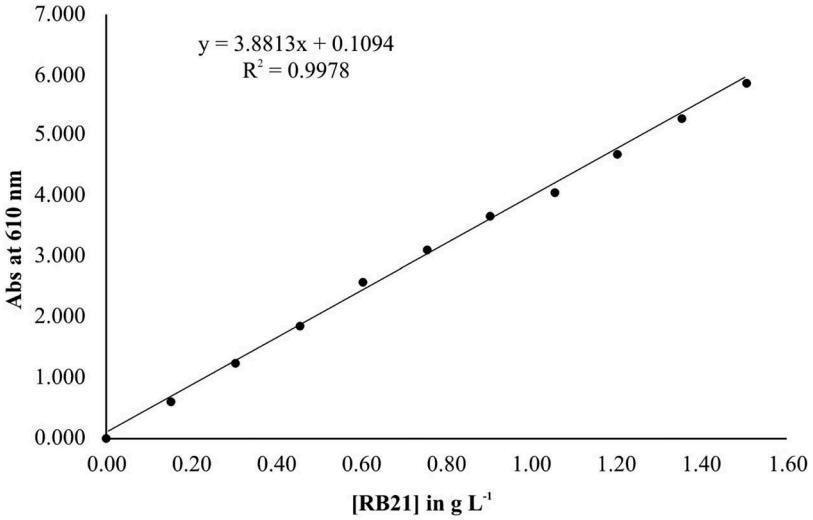

Figure 3. Calibration curve of RB21 concentration.

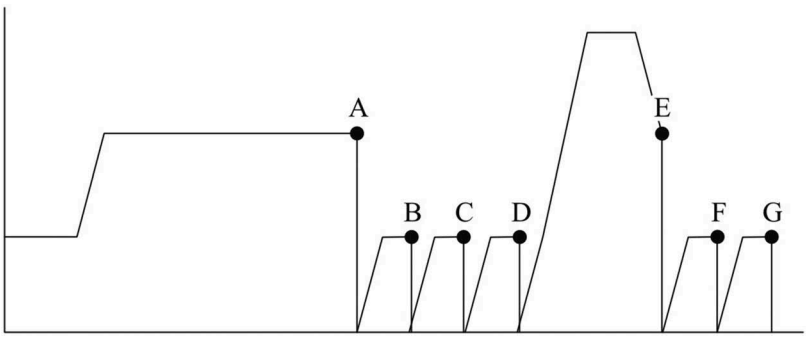

Figure 4. The dots represent the moments in which the baths were collected.

Samples from all seven steps (Figure 4) were collected and Abs were assessed by visible spectrophotometry, under illuminant D_{65}, 10º (Konica Minolta CM 3600d), in order to determinate RB21 concentrations, applying Equation 3.

Table 3. Planning matrix with K S^{-1} values.

N	X1	NaCl	X2	Na_2CO_3	X3	NaOH	K S^{-1} (exp.)	K S^{-1} (calc.)
1	−1	35	−1	7.5	−1	0.25	21.109	22.144
2	1	65	−1	7.5	−1	0.25	24.520	22.323
3	−1	35	1	12.5	−1	0.25	22.267	24.376
4	1	65	1	12.5	−1	0.25	25.891	25.503
5	−1	35	−1	7.5	1	0.75	22.485	23.836
6	1	65	−1	7.5	1	0.75	24.651	22.527
7	−1	35	1	12.5	1	0.75	22.052	23.828
8	1	65	1	12.5	1	0.75	25.051	24.325
9	−2	20	0	10	0	0.5	18.854	17.896
10	2	80	0	10	0	0.5	29.580	28.503
11	0	50	−2	5	0	0.5	22.820	23.636
12	0	50	2	15	0	0.5	24.891	23.230
13	0	50	0	10	−2	0	20.932	19.880
14	0	50	0	10	2	1	23.165	22.682
15	0	50	0	10	0	0.5	25.783	24.051
16	0	50	0	10	0	0.5	25.051	23.808
17	0	50	0	10	0	0.5	25.605	22.883

D_E modeling

In addition to the dyeing step, the following steps may also contain dyestuff residues, due to dyestuffs hydrolysis (Tang et al. 2018; Tian et al. 2018). Thus, adopting each sample as an "Abs/[RB21]" function (Equation 3), the [RB21] in the final effluent was calculated through Equation 4.

$$\frac{\partial Abs_f}{\partial [RB21]_f} = \int_{\partial_7}^{\partial_1} \frac{\partial Abs_n}{\partial [RB21]_n} \tag{4}$$

And the D_E is calculated through Equation 5.

$$\% \; E = \left\{ 1 - \left[\int_{\partial_7}^{\partial_1} \frac{\partial Abs_n}{\partial [RB21]_n} \cdot \left([RB21]_0 \right)^{-1} \right] \right\} \cdot 100 \tag{5}$$

Results and discussion

Table 3 presents the experimental planning applied during the assays, with all combinations of factors and their respective answers.

This data sheet was used to obtain the model by the least squares method. Similarities between experimental K S^{-1} coefficient values are observed when compared to the calculated K S^{-1} obtained by the model.

Figure 5 graphically displays the comparison of the experimental data to the data predicted by the model, where low data fluctuation is observed.

Table 4 presents the ANOVA analysis to the model shown in Equation 4, which was fitted to the experimental data.

The variance values were near 90%, and the multiple correlation value was close enough to the unit. This value obtained by the fitted multiple correlation indicates that the model is able to predict 79,85% of the experimental data with at a 95% of confidence level. The F_{Calc} value was approximately sevenfold higher than F_{Tab}, demonstrating the significance of the model and its adequate use on the prediction of K S^{-1} values under the studied conditions.

$$K \; S^{-1} = 21.5154 + 2.1038x_1 + 0.4139x_2 + 0.3071x_3 - 0.6033x_3^2 \tag{4}$$

Several authors have verified RSM as being able to contribute to predictions on the amount of dyestuffs present in coloration processes, such as Schabbach, Bondioli, and Fredel (2013), who have verified a linear increase of K S^{-1} with increasing pigment masses in ceramic glazes. Using ground

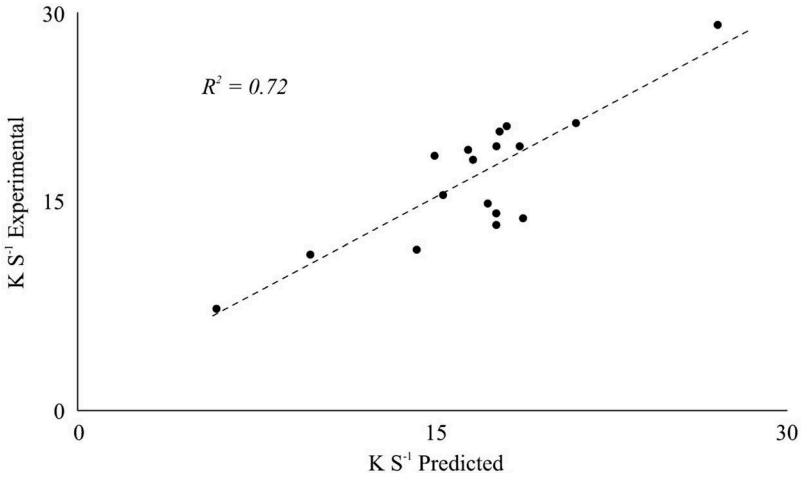

Figure 5. Correlation between experimental and predicted values of K S^{-1}.

Table 4. ANOVA with 95% of confidence level.

		ANOVA				
Results	Statistic	DF	SS	SA	F_{calc}	F_{tab}
Regression	-	10	83.9667	8.3967	20.6321	3.1300
Residual	-	6	6.8626	1.1438	-	
R multiple	0.9615			-		
R^2	0.9244					
R^2adjusted	0.7985					

calcium carbonate as a paper pigment, Bunkholt and Kleiv (2014) presented a linear model of the concentration (%) of 14 components of the dyestuff mixture measured by the K S^{-1} value.

According to Santana et al. (2018), the optimization is carried out by model fitting in combination to RSM, where the studied factors coexist from the analysis of each surface if an optimal condition for each factor is obtained. The RSM analysis of the present study is described in Figures 6–8.

The RSM indicates that higher Na_2CO_3 and NaCl values lead to higher K S^{-1} values. Higher NaCl values lead to higher K S^{-1} values, while NaOH does not have the same effect. Values near to the midpoint provide higher K S^{-1} values.

As observed in the previous RSM, higher Na_2CO_3 values lead to higher K S^{-1} values. NaOH displayed a similar effect as before, with values near to the midpoint provide higher K S^{-1} values.

Based on the equation generated by the model and RSM analysis, where the effects of all factors were assessed, the model formulation described in Table 5 was chosen for the application and eventually comparison to the formulation recommended by the dyestuff supplier, also displayed in Table 5.

The temperature and time were the same in both dyeings. The comparison was carried out through K S^{-1}, D_E, and colorfastness to water tests (ABNT 2013), as well as rubbing (ABNT 2007). The results, K S^{-1}, D_E, and colorfastness, are presented in Table 6.

Besides higher K S^{-1} values, the model presented D_E = 59.29, against the D_E = 53.30 value presented by the supplier, representing an economy of almost 6% of dyestuff.

The colorfastness to water and rubbing results are shown in Table 7, where similar colorfastness values are noted, indicating the model accuracy for dyeings with the RB21 dyestuff. The colorfastness scores between the experiments did not exceed a half point, on a scale where 5 indicates the best condition and 1 indicates the worst.

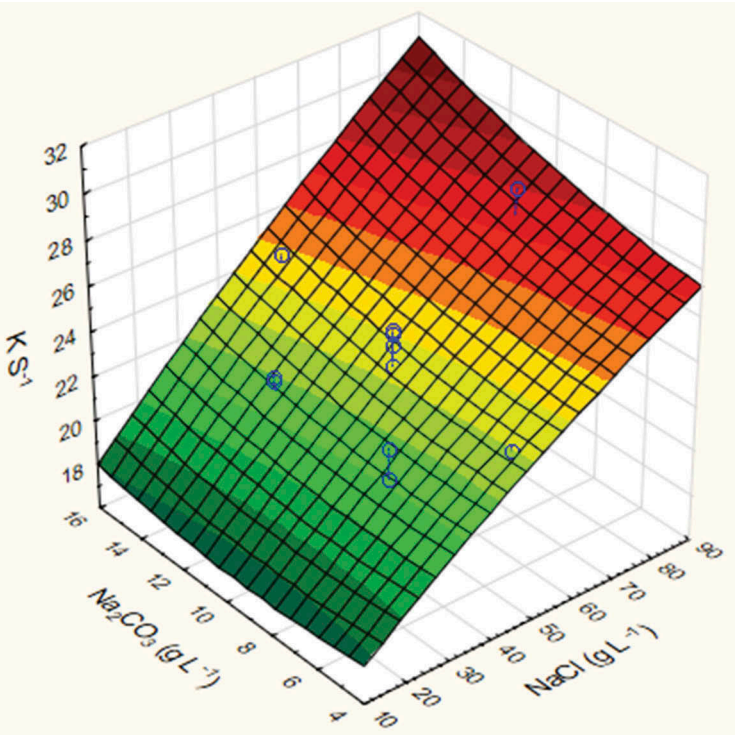

Figure 6. Combined effects of Na_2CO_3 and NaCl concentrations.

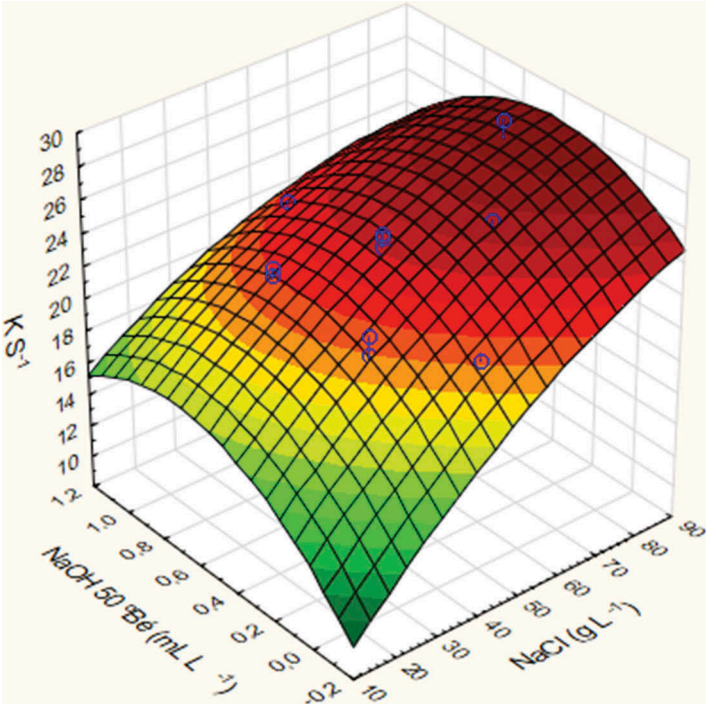

Figure 7. Combined effects of NaOH 50 ºBé and NaCl concentrations.

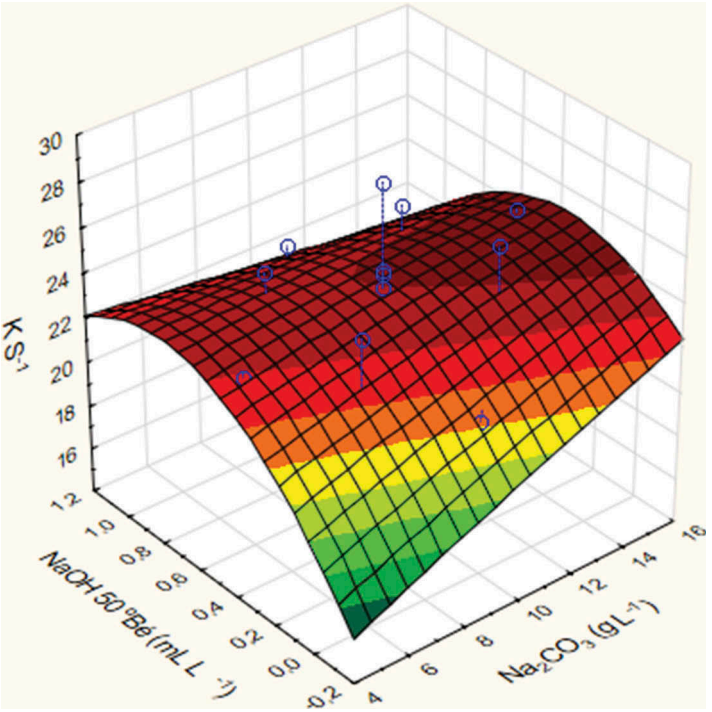

Figure 8. Combined effects of NaOH and Na_2CO_3.

Table 5. Model and supplier formulation recipes.

	Formulation	
Chemicals	Supplier	Model
RB21 (% owf)	1.50	1.50
NaCl (g L^{-1})	70.00	80.00
Na_2CO_3 (g L^{-1})	19.00	15.00
NaOH 50 ºBÉ (mL L^{-1})	1.00	0.83

Table 6. D_E values of dyeing with the model and supplier formulations.

	Bath								
g L^{-1}	A	B	C	D	E	F	G	K S^{-1}(exp.)	D_E (%)
Supplier	0.1451	0.0937	0.0255	0.0067	0.1294	0.0500	0.0165	23.28	53.30
Model	0.1451	0.0819	0.0126	0.0018	0.1225	0.0322	0.0111	29.48	59.29

Table 7. Model and supplier dyeing colorfastness.

		Supplier		Model	
Colorfastness		C	S	C	S
Water		4	3/4	4	4
Rubbing	Dry	4	-	4	-
	Wet	3/4	-	3/4	-

OBS = observation; C = color change; S = staining.

Conclusions

RSM is an adequate computational tool to support cotton dyeing processes with RB21 dyestuff. The best conditions for finding the highest K S^{-1} values apply an NaCl concentration of 80 g L^{-1}, an Na_2CO_3 concentration of 15 g L^{-1}, and an NaOH 50 ºBé concentration of 0.83 mL L^{-1}.

The application of the model led to a 6% increase in D_E. The economy obtained for dyeing 100 kg of cotton with RB21 in the model conditions could be up to US$0.78, under the same colorfastness conditions. Therefore, the use of RSM is proven adequate in color matching and can contribute to the textile industry for the prediction or formulation of a specific color.

Acknowledgments

The authors are grateful to CNPq, Golden Technology, and SENAI-SP Research Support Program.

Funding

This work was supported by the Conselho Nacional de Desenvolvimento Científico e Tecnológico.

ORCID

Jorge Marcos Rosa http://orcid.org/0000-0003-1351-5516
Sueli Ivone Borrely http://orcid.org/0000-0002-9692-5539

References

ABNT. 2007. *Textiles – tests for colour fastness part X 12: Colour fastness to rubbing*. São Paulo: Associação Brasileira de Normas Técnicas.

ABNT. 2013. *Textiles – tests for colour fastness part E01: Colour fastness to water*. São Paulo: Associação Brasileira de Normas Técnicas.

Benvenga, C., M. Antônio, A. F. H. Librantz, J. C. C. Santana, and E. B. Tambourgi. 2016. Genetic algorithm applied to study of the economic viability of alcohol production from cassava root from 2002 to 2013. *Journal of Cleaner Production* 113:483–94. doi:10.1016/j.jclepro.2015.11.051.

Bordin E. R., Camargo A. F., Rossetto V., Scapini T., Modkovski T. A., Weirich S., Carezia C., Franceschetti M. B., Balem A., Golunski S. M., et al. Non-toxic bioherbicides obtained from *Trichoderma koningiopsis* can be applied to the control of weeds in agriculture crops. *Industrial Biotechnology* 14 (3):157–63. doi:10.1089/ind.2018.0007.

Bunkholt, I., and R. A. Kleiv. 2014. The applicability of the Kubelka–Munk model in GCC brightness prediction. *Minerals Engineering* 56:129–35. doi:10.1016/j.mineng.2013.11.009.

Das, A., and S. Mishra. 2017. Removal of textile dye reactive green-19 using bacterial consortium: process optimization using response surface methodology and kinetics study. *Journal of Environmental Chemical Engineering* 5 (1):612–27. doi:10.1016/j.jece.2016.10.005.

Ezekannagha, C. B., C. N. Ude, and O. D. Onukwuli. 2017. Optimization of the methanolysis of lard oil in the production of biodiesel with response surface methodology. *Egyptian Journal of Petroleum* 26 (4):1001–11. doi:10.1016/j.ejpe.2016.12.004.

Farzana, N., M. Z. Uddin, M. M. Haque, and A. N. M. A. Haque. 2018, November 1–15. Dyeability, kinetics and physico-chemical aspects of *Bombyx mori* muslin silk fabric with bi-functional reactive dyes. *Journal of Natural Fibers*:1–15. doi:10.1080/15440478.2018.1546638.

Hallas, G. 2002. Chemistry of anthraquinonoid, polycyclic and miscellaneous colorants. In *Colorants and auxiliaries*, ed. J. Shore, 960. 2nd ed. Hampshire: SDC - Society of Dyers and Colourists.

Ma, Q., and L. Wang. 2015. Adsorption of Reactive Blue 21 onto functionalized cellulose under ultrasonic pretreatment: kinetic and equilibrium study. *Journal of the Taiwan Institute of Chemical Engineers* 50 (May):229–35. doi:10.1016/J.JTICE.2014.12.018.

Mokhtar, N. M., W. J. Lau, A. F. Ismail, S. Kartohardjono, S. O. Lai, and H. C. Teoh. 2016. The potential of direct contact membrane distillation for industrial textile wastewater treatment using PVDF-cloisite 15A nanocomposite membrane. *Chemical Engineering Research and Design* 111:284–93. doi:10.1016/j.cherd.2016.05.018.

Ngwabebhoh, F. A., M. Gazi, and A. A. Oladipo. 2016. Adsorptive removal of multi-azo dye from aqueous phase using a semi-IPN superabsorbent chitosan-starch hydrogel. *Chemical Engineering Research and Design* 112:274–88. doi:10.1016/j.cherd.2016.06.023.

Prado, M. V. 2018. *Sectorial report of Brazilian textile industry*. São Paulo: Instituto de Estudos e Marketing Industrial (IEMI).

Rosa, J. M., and A. M. F. Fileti. 2016. Applying of an artificial neural network in dyeings of cotton with reactive black 5 dyestuff. In *Modelling, simulation and identification: intelligent systems and control*, A. M. F. Fileti and F. V. Silva. ed., Campinas: ACTA Press, 4–343. doi:10.2316/P.2016.841-019.

Rosa, J. M., A. M. F. Fileti, E. B. Tambourgi, and J. C. C. Santana. 2015. Dyeing of cotton with reactive dyestuffs: the continuous reuse of textile wastewater effluent treated by ultraviolet/hydrogen peroxide homogeneous photocatalysis. *Journal of Cleaner Production* 90. doi:10.1016/j.jclepro.2014.11.043.

Rosa, J. M., E. B. Tambourgi, J. C. C. Santana, M. de Campos Araujo, W. C. Ming, and N. Trindade. 2014. Development of colors with sustainability: a comparative study between dyeing of cotton with reactive and vat dyestuffs. *Textile Research Journal* 84:10. doi:10.1177/0040517513517962.

Santana, J., C. Carlos, S. A. Araújo, W. A. L. Alves, P. A. Belan, L. Jiangang, C. Jianchu, and L. Dong-Hong. 2018. Optimization of vacuum cooling treatment of postharvest broccoli using response surface methodology combined with genetic algorithm technique. *Computers and Electronics in Agriculture* 144:209–15. doi:10.1016/j.compag.2017.12.010.

Sathish, S., and S. Vivekanandan. 2016. Parametric optimization for floating drum anaerobic bio-digester using response surface methodology and artificial neural network. *Alexandria Engineering Journal* 55 (4):3297–307. doi:10.1016/j.aej.2016.08.010.

Schabbach, L. M., F. Bondioli, and M. C. Fredel. 2013. Color prediction with simplified Kubelka–Munk model in glazes containing Fe2O3–ZrSiO4 coral pink pigments. *Dyes and Pigments* 99 (3):1029–35. doi:10.1016/j.dyepig.2013.08.009.

Shen, J., L. Ya, and H. Ji-Huan. 2016. On the Kubelka–Munk absorption coefficient. *Dyes and Pigments* 127:187–88. doi:10.1016/j.dyepig.2015.11.029.

Shu, D., K. Fang, X. Liu, Y. Cai, X. Zhang, and J. Zhang. 2018. Cleaner coloration of cotton fabric with reactive dyes using a pad-batch-steam dyeing process. *Journal of Cleaner Production* 196:935–42. doi:10.1016/j.jclepro.2018.06.080.

Siddiqua, U. H., S. Ali, M. Iqbal, and T. Hussain. 2017. Relationship between structure and dyeing properties of reactive dyes for cotton dyeing. *Journal of Molecular Liquids* 241 (September):839–44. doi:10.1016/J.MOLLIQ.2017.04.057.

Tang, A. Y., C. H. Lee, Y. M. Wang, and C. W. Kan. 2018. Dyeing cotton with reactive dyes: a comparison between conventional water-based and solvent-assisted PEG-based reverse micellar dyeing systems. *Cellulose*. doi:10.1007/s10570-018-2150-3.

Tian, X., F. Hua, C. Lou, and X. Jiang. 2018. Cationic cellulose nanocrystals (CCNCs) and chitosan nanocomposite films filled with CCNCs for removal of reactive dyes from aqueous solutions. *Cellulose* 25 (7):3927–39. doi:10.1007/s10570-018-1842-z.

Torbati, S., A. R. Khataee, and A. Movafeghi. 2014. Application of watercress (*Nasturtium officinale* R. Br.) for biotreatment of a textile dye: investigation of some physiological responses and effects of operational parameters. *Chemical Engineering Research and Design* 92 (10):1934–41. doi:10.1016/j.cherd.2014.04.022.

Vanaamudan, A., B. Chavada, and P. Padmaja. 2016. Adsorption of Reactive Blue 21 and reactive red 141 from aqueous solutions onto hydrotalcite. *Journal of Environmental Chemical Engineering* 4 (3):2617–27. doi:10.1016/J.JECE.2016.04.039.

Vanaamudan, A., N. Pathan, and P. Pamidimukkala. 2014. Adsorption of Reactive Blue 21 from aqueous solutions onto clay, activated clay, and modified clay. *Desalination and Water Treatment* 52 (7–9):1589–99. doi:10.1080/19443994.2013.789405.

Zollinger, H. 2003. *Color chemistry: syntheses, properties and applications of organic dyes and pigments*. 3rd ed. Cambridge: Wiley-VCH.

Zurita Ares, M. C., Villa González, E., Torres Gómes, A. I., Fernández, J. M. 2014. An easy method to estimate the concentration of mineral pigments in colored mortars. *Dyes and Pigments* 101: 329–37. doi.10.1016/j.dyepig.2013.10.001.